Role of *C*-Terminal Region of Yeast ADP/ATP Carrier 2 Protein: Dynamics of Flexible *C*-Terminal Arm

KAZUTO OHKURA[1], HITOSHI HORI[2] and YASUO SHINOHARA[3]

[1]*Faculty of Pharmacy, Chiba Institute of Science, Choshi, Chiba;*
[2]*Department of Biological Science and Technology, Faculty of Engineering, and*
[3]*Institute for Genome Research, The University of Tokushima, Tokushima, Japan*

Abstract. *Background: The ADP/ATP carrier catalyzes the exchange of ADP and ATP across the inner mitochondrial membrane. Materials and Methods: The molecular dynamics of modeled yeast type 2 AAC (yAAC2) was analyzed and molecular parameters were determined. Results: The yAAC2 C-terminal moved flexibly and a negative electrostatic potential field (ESP) was located in the C-terminal region. The ESP field is always located in the C-terminal area during C-terminal truncation (d1-d9). Further C-terminal truncation occurred on field invagination into the core region (d11, d14, d16). The 2-6 C-terminal amino acid truncation did not affect the biological activity. The d7-d9 truncated mutants lost their biological function. Conclusion: A critical point in yAAC2 function was shown between d6 and d7 C-terminal truncation. The C-terminal structure of yAAC2 is thought to be involved in biological function control.*

The ADP/ATP carrier (AAC) is the most abundant protein in the mitochondrial carrier, catalyzing the exchange of ADP and ATP across the inner mitochondrial membrane (1). AAC has a 6-transmembrane structure in the inner mitochondrial membrane, and *N*- and *C*-terminals exposed to the cytosolic side (2). The crystal structure of bovine type 1 AAC (bAAC1) in a complex with carboxyatractyloside (CATR) was examined, and its predicted topology in the mitochondrial membrane was validated (3). However, the dynamics of AAC have not yet been clarified. Thus, analysis of the structure/function relationship is required to confirm the molecular features of AAC. In the present study, we modeled the yeast type 2 AAC (yAAC2) molecule based on bAAC1 X-ray data and examined its molecular dynamics. The *N*- and *C*-terminals of yAAC2 are longer than those of bAAC1 and the additional region seems to be concerned with AAC function (4). Previously, we reported the role of the yAAC2 *C*-terminal in nucleotide transport using *C*-terminal-truncated yAAC2 mutants. Furthermore, the water accessibility of the C-terminal region of yAAC2 has been examined using site-directed mutagenesis and chemical modification techniques (4). In this presentation, we modeled the *C*-terminal-truncated yAAC2 molecules and analyzed their molecular features regarding their biological activity.

Correspondence to: Dr. Kazuto Ohkura, Faculty of Pharmacy, Chiba Institute of Science, 3 Shiomi-cho, Choshi, Chiba, 288-0025, Japan. Tel: +81 479304785, Fax: +81 479304785, e-mail: kohkura@sag.bekkoame.ne.jp

Key Words: ADP/ATP carrier, molecular dynamics, yAAC2 function.

Materials and Methods

Modeling and structure analysis of yeast ADP/ATP carrier. Molecular modeling of yeast ADP/ATP carrier 2 (yAAC2) was performed based on the Protein Data Bank (PDB) data of bovine heart AAC 1 (bAAC1; 1OKC) (5, 6). Molecular dynamics (MD) analysis of minimized yAAC2 was performed and the yAAC2 conformers obtained. Molecular orbital (MO) analysis of each MD conformer-derived *C*-terminal peptide (M^{304}-F^{317}: removed a distorted *C*-terminal Lys^{318}) were performed (7, 8). Electrostatic potential (EPS) fields of C-terminal-truncated yAAC2s were calculated and the –1.0 kT/e contour was displayed as a cloud. The various lengths of *C*-terminal peptides (M^{304}-K^{318}) were extracted from minimized yAAC2 and their MO parameters analyzed (5, 6, 8).

Function analysis of yAAC2. The cDNA fragment encoding yAAC2 was prepared as described elsewhere (2, 9). Using this cDNA as template, we prepared cDNAs encoding *C*-terminal-truncated mutants of yAAC2 by PCR. Biological responses of *C*-terminal truncated yAAC2 in WB-12 cells was examined using YPD and YPGly plate assay (4).

Results

Modeling and dynamics of yAAC2. A comparison of the amino acid sequence of yAAC2 with that of bAAC1 revealed that the *N*- and *C*-terminals of yAAC2 are 15 and 6 amino acids longer, respectively, than those of bAAC1. The *N*- and *C*-terminals of the yAAC2 molecule moved flexibly during MD simulation, while the core region

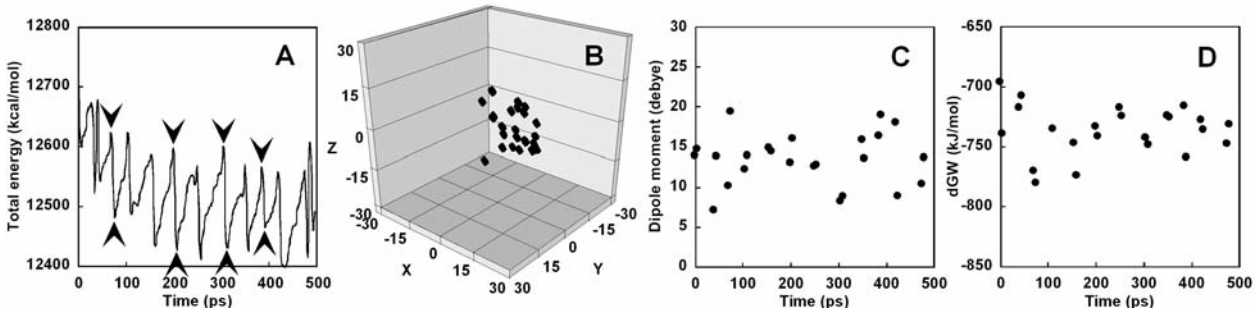

Figure 1. *Dynamics analysis of modeled yAAC2. A, Total energy of yAAC2 during MD simulation. B, Dipole moment (in vacuum conditions) directions of C-terminal peptides (M^{304}-F^{317}), which were extracted from MD conformers (e.g. arrows in 1A). C, Dipole moment values from 1B. D, Solvation free energies of C-terminal peptides.*

remained mostly still. The total energy profile of yAAC2 during MD simulation fluctuated (12400-12770 kcal/mol) and gradually decreased (Figure 1A). The molecular features of the *C*-terminal involving 14 peptides (M^{304}-F^{317}) during MD analysis were examined using MO parameters. The *C*-terminal peptide dipole moments at maximal or minimal energy points, indicated by the arrows in Figure 1A, showed a similar direction (Figure 1B), and their intensities were 7.077-19.405 D (Figure 1C). The solvation free energy (dGW: the stereo-hydrophobic parameter (6)) of *C*-terminal peptides changed over the range from –780.4 to –696.4 kJ/mol (Figure 1D).

Effect of C-terminal structure on biological function and electrostatic potential field. The 2-6 *C*-terminal truncated (d2-d6) yAAC2 mutants-transformed WB-12 cells were viable on both YPD and YPGly plates (Table I). The d7-d9 mutant-transformed cells were viable on YPD, but inviable on YPGly plates. To understand the *C*-terminal truncation regarding the molecular features, ESP analysis was performed. The modeled yAAC2 expressed a negative electrostatic potential field in the *C*-terminal region (d0: Figure 2). The negative field was always located in the *C*-terminal area during *C*-amino acid truncation (d1-d9) as shown in d3, d6 and d7 in Figure 2. Further *C*-terminal truncation occurred in the field invagination into the core region; the shapes are shown in d11, d14 and d16 of Figure 2.

Molecular features of yAAC2 C-terminal. The molecular features of *C*-terminal peptides, derived from the M^{304}-K^{318} region, were examined using MO analysis. The dipole moments of these peptides were directed in almost the same way (Figure 3A), and their intensities tended to increase (3.427-8.446 D) with amino acid length (Figure 3B). The stereo-hydrophobic parameter (dGW) of these peptides decreased with amino acid length (from –708.5 to –156.7 kJ/mol) (Figure 3C).

Table I. *Function of C-terminal-truncated yAAC2.*

Sample	YPD	YPGly
wt	+	+
WB-12	+	–
d2	+	+
d4	+	+
d5	+	+
d6	+	+
d7	+	–
d8	+	–
d9	+	–

Viability (+: viable, –: inviable) of transformants expressing various yAAC2 mutants on YPD or YPGly plates. The plates were incubated at 30˚C for 5 days. WB-12, yeast cells lacking functional *AAC1* and *AAC2* genes; wt, WB-12 cells expressing wild-type yAAC2; dn (d2-d9), WB-12 cells expressing yAAC2 mutant lacking C-terminal n amino acids.

Discussion

The functional importance of the *C*-terminal region of AAC was reported previously (10); however, molecular dynamics analysis regarding the structure and function of the *C*-terminal region has not been performed. The *N*- and *C*-terminal regions of yAAC2 markedly fluctuated during MD simulation. On the other hand, the core region of yAAC2 did not fluctuate during the MD simulation period. This observation is consistent with the fact that the core region exists in the inner mitochondrial membrane and its structure does not dynamically change. The ESP field is one of the important parameters regarding molecular features and it affects reactivity toward external substrates. The yAAC2 molecule showed a negative field in the *C*-terminal region, and the field always occupied the *C*-terminal amino acid in *C*-terminal truncated models (d1-d7, Figure 2). When 11 or more amino acids were truncated from the C-terminal (*e.g.*

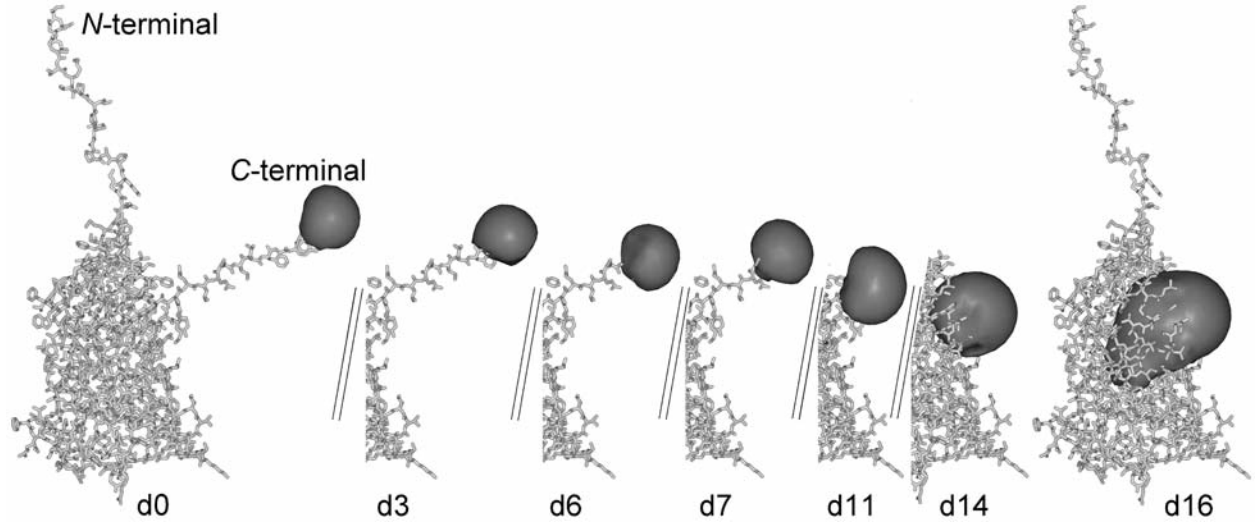

Figure 2. *Electrostatic potential field of yAAC2. Negative ESP fields of modeled yAAC2 (d0) and C-terminal-truncated models (d3-d16) are shown as clouds. The –1.0 kT/e contour of ESP is displayed as a cloud.*

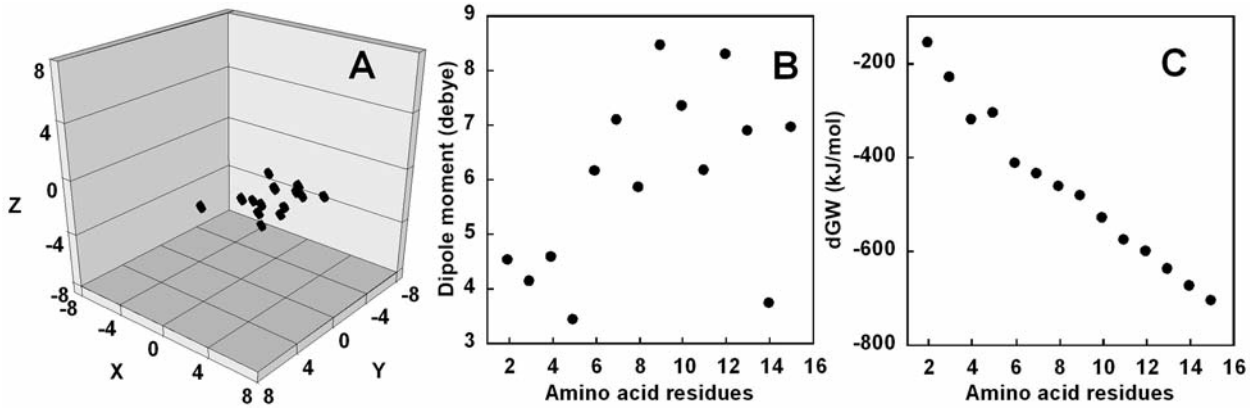

Figure 3. *MO parameters of C-terminal peptides. The 14 C-terminal involved peptides were extracted from z-matrix data of M^{304}-K^{318} (MY^{305}, MYD^{306}, $MYDQ^{307}$, $MYDQL^{308}$, $MYDQLQ^{309}$, MYDQLQM310, $MYDQLQMI^{311}$, $MYDQLQMIL^{312}$, $MYDQLQMILF^{313}$, $MYDQLQMILFG^{314}$, $MYDQLQMILFGK^{315}$, $MYDQLQMILFGKK^{316}$, $MYDQLQMILFGKKF^{317}$, $MYDQLQMILFGKKFK^{318}$). Dipole moment (in vacuum conditions) directions (A), values (B) and solvation free energies (C) of these peptides.*

d11, d14 and d16), the ESP field gradually penetrated into the core region. The yAAC2 function was maintained by 6 amino acid truncation, but the function was lost by the truncation of 7 or more amino acids from the *C*-terminal. In the d7 mutant, the ESP field seems to interfere with the core region, and yAAC2 loses its transport function. Thus, the *C*-terminal structure of the yAAC2 molecule is thought to be involved with biological function control. The *C*-terminal structure dynamically fluctuated together with the ESP field and this ESP-associated movement seems to control the ADP/ATP transport activity. We then examined the correlation between the ESP profile and biological activity using *C*-terminal-truncated mutants. Each dipole moment of *C*-terminal-derived peptide (residue no. 2-15, Figure 3) was directed in the same way. The moment profile did not differ between the d6- and d7-mutants, as in the case of the ESP profile. Further molecular analysis is being conducted regarding the ESP involved in the structural change in substrate recognition.

In our previous report, we constructed various single Cys yAAC2 mutants in the region of the amino acids Gly^{287}-Lys^{318}, and performed topological analysis (4). The

continuous M310C-K318C region showed high-level reactivity with eosin-5-maleimide (EMA) regardless of the presence of carboxyatractyloside (CATR) or bongkrekic acid (BKA); these regions were projecting from the membrane and the transmembrane water-accessible residues were assigned as Gly^{298}, Ala^{299}, Ile^{302}, Tyr^{305} and Asp^{306}. In the functional analysis of *C*-terminal truncated mutants, the *C*-terminal ESP field seems to affect the water accessibility of the transmembrane core, so certain yAAC2 mutants (*e.g.* d7, d11, d14 and d16; Figure 2) may lose their transport function. The critical ESP point concerning biological function may exist halfway between the d6 and d7 ESP field. Moreover, in CATR or BKA-associated fixed yAAC2 structures, water accessibility seems to affect the reactivity of the *C*-terminal region to EMA. Thus, a detailed analysis of *C*-terminal ESP control is required. Controlling the *C*-terminal function of yAAC2 may lead to the control of energy metabolism through ATP synthesis. The development of energy metabolism-modifying drugs for body weight control is eagerly anticipated. The molecular design of *C*-terminal regulatory compounds is currently underway using dynamics analysis of the AAC *C*-terminal region.

References

1 Nury H, Dahout-Gonzalez C, Trezeguet V, Lauquin GJ, Brandolin G and Pebay-Peyroula E: Relations between structure and function of the mitochondrial ADP/ATP carrier. Annu Rev Biochem *75*: 713-741, 2006.

2 Hatanaka T, Kihira Y, Shinohara Y, Majima E and Terada H: Characterization of loops of the yeast mitochondrial ADP/ATP carrier facing the cytosol by site-directed mutagenesis. Biochem Biophys Res Commun *286*: 936-942, 2001.

3 Pebay-Peyroula E, Dahout-Gonzalez C, Kahn R, Trezeguet V, Lauquin GJM and Brandolin G: Structure of mitochondrial ADP/ATP carrier in complex with carboxyatractyloside. Nature *426*: 39-44, 2003.

4 Iwahashi A, Ishii A, Yamazaki N, Hashimoto M, Ohkura K, Kataoka M, Majima E, Terada H and Shinohara Y: Functionally important conserved length of *C*-terminal regions of yeast and bovine ADP/ATP carriers, identified by deletion mutants studies, and water accessibility of the amino acids at the *C*-terminal region of the yeast carrier. Mitochondrion *8*: 196-204, 2008.

5 Ohkura K, Nagamune H and Kourai H: Structural analysis of human specific cytolysin intermedilysin aiming application to cancer immunotherapy. Anticancer Res *24*: 3343-3354, 2004.

6 Ohkura K: Exploring unique structures: Flexibility is a significant factor in biological activity. Biol Pharm Bull *30*: 1025-1036, 2007.

7 Ohkura K, Hori H and Nagamune H: Molecular dynamics of human-specific cytolysin: analysis of membrane binding motif for therapeutic application. Anticancer Res *26*: 4055-4062, 2006.

8 Ohkura K, Sukeno A, Nagamune H and Kourai H: Bridge-linked *bis*-quaternary ammonium anti-microbial agents: relationship between cytotoxicity and anti-bacterial activity of 5,5'-[2,2'-(tetramethylenedicarbonyldioxy)-diethyl]*bis* (3-alkyl-4-methyl-thiazonium iodide)s. Bioorg Med Chem *13*: 2579-2587, 2005.

9 Hashimoto M, Shinohara Y, Majima E, Hatanaka T, Yamazaki N and Terada H: Expression of the bovine heart mitochondrial ADP/ATP carrier in yeast mitochondria: significantly enhanced expression by replacement of the *N*-terminal region of the bovine carrier by the corresponding regions of the yeast carriers. Biochim Biophys Acta *1409*: 113-124, 1999.

10 Aquila H, Misra D, Eulitz M and Klingenberg M: Complete amino acid sequence of the ADP/ATP carrier from beef heart mitochondria. Hoppe Seylers Z Physiol Chem *363*: 345-349, 1982.

Received April 28, 2009
Revised July 15, 2009
Accepted July 20, 2009